Eun-chae Jeon
e-mail: purelife@plaza.snu.ac.kr
School of Materials Science and Engineering,
Seoul National University,
Seoul, 151-742,
Korea

Joo-Seung Park
e-mail: joospark@ats.go.kr
Dept. of Manufacturing Technology and Standards,
Korea Agency for Technology and Standards,
Gwacheon, 427-716,
Korea

Dongil Kwon
e-mail: dongilk@snu.ac.kr
School of Materials Science and Engineering,
Seoul National University,
Seoul, 151-742,
Korea

Statistical Analysis of Experimental Parameters in Continuous Indentation Tests Using Taguchi Method

The continuous indentation test, which applies an indentation load to a material and records the indentation depth, yields indentation tensile properties whose accuracy can vary depending on such experimental parameters as number of unloadings, unloading ratio, maximum depth ratio and indenter radius. The Taguchi method was used to quantify their effects and to determine their optimum values. Using signal-to-noise ratio calculated from the error in the indentation tensile properties, the criterions and the optimum values for the experimental parameters were presented. The indentation tensile properties evaluated with the optimum parameters were in better agreement with the tensile properties.
[DOI: 10.1115/1.1605115]

I Introduction

The continuous indentation test is widely used recently due to its various merits. During the test the load is applied to a material with an indenter, and the load and the indentation depth are recorded simultaneously. The simplest load-depth curve is present in Fig. 1, which includes one loading curve and one unloading curve. The maximum depth, $h_{\max}$, is the total displacement of the material and the indenter at the maximum load, $P_{\max}$, including the elastic and plastic deformation. When unloading, the elastic deformation is fully recovered and the initial slope of the unloading curve is the indentation stiffness of the specimen and the indenter, S [1,2]. Therefore, the final depth, h_f, means the plastic deformation of the material.

Doerner and Nix [2] showed that elastic modulus could be evaluated by this test, and Oliver and Pharr [1] settled a method to evaluate elastic modulus and load-on hardness. However, it is going on progress to evaluate the other mechanical properties such as fracture toughness [3,4], tensile properties [5,6], viscoelastic properties [7,8] and residual stress [9,10]. Among them, the methods to evaluate tensile properties are being tried to use in some industrial fields because they can be applied to materials with local property gradients and to materials in use that cannot be applied for uniaxial tensile test. In addition to that, the standardization of the method is being tried.

However, the methods require some unloading procedures in a test as shown in Fig. 2 due to the calibration of the contact depth and the iteration procedure explained later. Several experimental parameters should be determined before the actual test whose effects on numerical calculations are not researched quantitatively in previous researches [5,6]. They showed the theoretical analysis only and ignored the effects of the experimental parameters on the tensile properties evaluated by the continuous indentation test, which are defined as the indentation tensile properties in this study. However, it is observed experimentally that the indentation tensile properties vary with the experimental parameters. Therefore, the research about their effects and their optimum values for accurate results is needed in order to use in industrial fields and to legislate a standard.

Contributed by the Materials Division for publication in the JOURNAL OF ENGINEERING MATERIALS AND TECHNOLOGY. Manuscript received by the Materials Division January 10, 2003; revision received June 17, 2003. Associate Editor: A. Pelegri and A. Karlsson.

In this study, the Taguchi method was applied to analyze the effects of the experimental parameters on the accuracy of the indentation tensile properties quantitatively, and the criterions and the optimum values for evaluating the exact indentation tensile properties were presented. Finally, the indentation tensile properties evaluated with the optimum values were compared with the results of uniaxial tensile tests in order to verify the validity of this study.

II Theoretical Background

2.1 Evaluation of Indentation Tensile Properties. The method used here to evaluate the indentation tensile properties is based on the study of Ahn and Kwon [5]. The strain is derived by differentiating the displacement in the depth direction. By multiplying by a constant, α=0.12, we can obtain the true strain [5]:

$$\varepsilon = \frac{\alpha}{\sqrt{1-(a/R)^2}} \frac{a}{R}, \tag{1}$$

where R is the indenter radius and a is a contact radius. Several researchers showed that the true stress is proportional to mean contact pressure in the fully plastic stage [5,6,11,12]:

$$\sigma = \frac{1}{\Psi} \frac{P}{\pi a^2}, \tag{2}$$

where P is the indentation load and the value of ψ, plastic constraint factor, is about 3.5.

The contact radius a in Eq. (1) and Eq. (2) can be calculated from the contact depth for a given ball indenter. The contact depth must be calibrated by taking elastic deflection and pile-up/sink-in into account. The contact depth as affected by the elastic deflection, h_c^*, can be obtained by calculating the initial slope of the unloading curves, i.e., [1]

$$h_c^* = h_{\max} - \omega \frac{P_{\max}}{S}. \tag{3}$$

Pile-up/sink-in can be calibrated by [13,14]

$$a^2 = \frac{5}{2} \frac{(2-n)}{(4+n)} a_*^2, \tag{4}$$

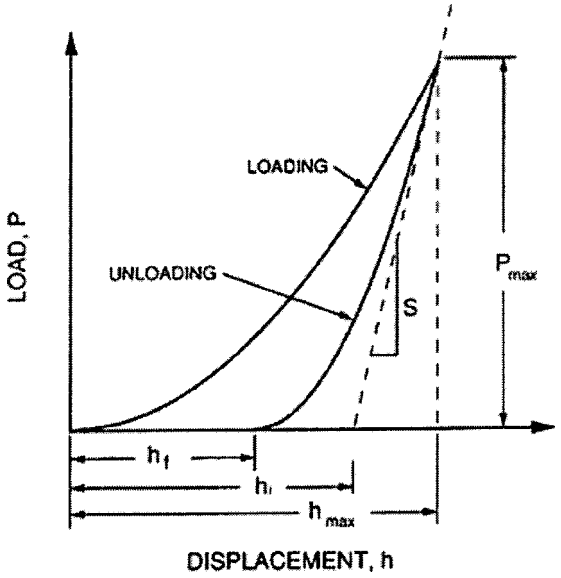

Fig. 1 The simplest load-depth curve of continuous indentation test

where a_* is the contact radius calculated from h_c^* and n is the work-hardening exponent.

The true strain and the true stress calculated by Eq. (1) and Eq. (2) are inserted into

$$\sigma = K\varepsilon^n, \tag{5}$$

where K is a strength coefficient [15]. The iteration is performed until n in Eq. (4) and Eq. (5) are the same. After K and n are determined, the constitutive equation in the fully plastic regime can be obtained. The yield strain is assumed 0.01, which was determined experimentally [16] and the tensile strain is assumed to be same with the work-hardening exponent [15]. The yield strength and the tensile strength are calculated by inputting these two strains in Eq. (5).

2.2 Experimental Parameters in Continuous Indentation Test. As indicated, the methods [5,6] require some unloading procedures in a test as shown in Fig. 2. Generally, the load is removed not totally but partially in order to reduce the testing time. They can be alternated how many there are the unloading curves and how much the load is partially removed. It is also important how much the indenter moves down in a material because that is directly related to the range of the true strain as shown in Eq. (1). It is also essential to determine how much the size of the indenter is.

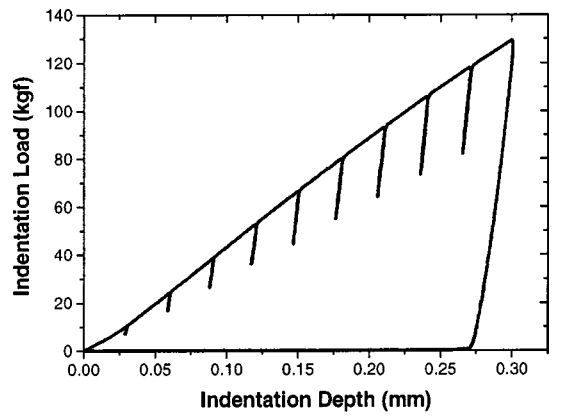

Fig. 2 General load-depth curve for evaluation of indentation tensile properties

Table 1 Experimental schedule based on the Taguchi method

No.	Number of unloadings	Maximum depth ratio	Indenter radius (mm)	Unloading ratio (%)
1	15	0.5	0.5	50
2	15	0.4	0.25	100
3	15	0.6	0.375	30
4	7	0.5	0.25	30
5	7	0.4	0.375	50
6	7	0.6	0.5	100
7	10	0.5	0.375	100
8	10	0.4	0.5	30
9	10	0.6	0.25	50

These four kinds of the experimental parameters are named as number of unloadings, unloading ratio, maximum depth ratio and indenter radius, respectively. The unloading ratio is the ratio of the unloading curve to the full unloading curve. The maximum depth ratio is the ratio of the maximum depth to the indenter radius, h_{max}/R. These four parameters are essential in building the general load-depth curve in Fig. 2 to evaluate the indentation tensile properties, and expected to have strong relationships to variables in the calculation of the load-depth curve such as the true stress, the true strain, the indentation stiffness, the strength coefficient and the work-hardening exponent. They are thus the most important experimental parameters affecting the accuracy of the indentation tensile properties.

2.3 Taguchi Method. Studying the effects of experimental parameters requires many experiments, much time and some certain statistical techniques for quantitative evaluation of the effects. Various design-of-experiment (DOE) methods are widely used to reduce this problem. DOE methods set up the efficient experimental schedule and produce a statistical analysis to indicate quickly and easily what parameters are important for the final results.

In particular, the Taguchi method is one of the most powerful DOE methods for experiments [17]. The method has been used popularly in the various fields, especially in the development of new products or the quality control. The method builds the most effective experimental schedules using orthogonal tables, and analyzes data easily and effectively with the signal-to-noise (SN) ratio:

$$SN = \frac{\text{Signal}}{\text{Noise}}. \tag{6}$$

In general, we get a better signal when the noise is smaller, so that a larger SN ratio yields better final results. Increasing the SN ratio makes the final results more desirable. That means the divergence of the final results becomes smaller. This is the most important feature of the SN ratio and the Taguchi method.

The method requires some experiences about the study and the experiments when the ranges of parameters are determined. It is recommended to set relatively large ranges with two or three levels in the first time such as to use a net having large mesh size. After confirming important parameters and ranges, the experimental schedule is built using small ranges with many levels. Another special feature of the method is that the interaction among the parameters is generally ignored for convenience. Though the effects of parameters can be misconstrued due to ignoring interactions, the optimum values determined by the method are always reasonable [17].

III Experimental Procedures

Using the Taguchi method, the experimental schedule was built using the $L_9(3^4)$ orthogonal table shown in Table 1. All values

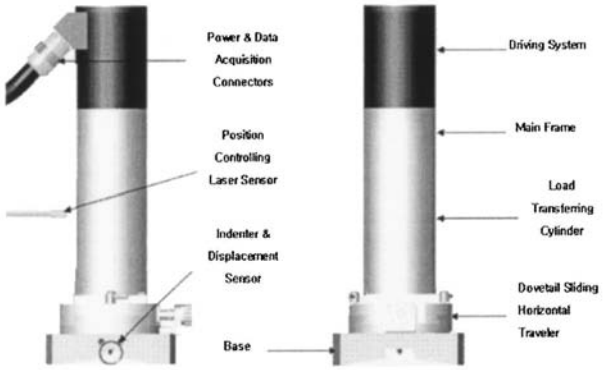

Fig. 3 Testing apparatus for continuous indentation test

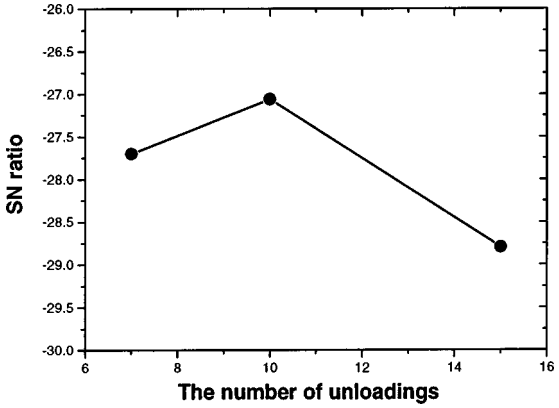

Fig. 4 *SN* ratio of the number of unloadings

were randomly arrayed according to the rule of the orthogonal table. Use of the Taguchi method can reduce the number of experiments necessary by almost 90 percent.

The materials tested were SCM400 steel, STD61 steel, SK3 steel, A335-P12 steel, A335-P91 steel, KP5 steel, and A106 steel, all popular industrial steels. The specimens were cut to 25 $\times$25$\times$20 mm, ground and polished with 1 μm alumina. Continuous indentation tests were performed for each material according to Table 1 using Frontics, Inc.'s AIS2000 equipment (see Fig. 3). To confirm reproducibility of the load-depth curves, the same experiments were repeated three times. The indentation tensile properties were obtained by analyzing the load-depth curves according to Ahn and Kwon's study [5]. Uniaxial tensile tests were also performed using an Instron 5582 to compare the results with the indentation tensile properties.

IV Results and Discussion

The tensile curves of all materials showed very high reproducibility. The tensile properties are shown in Table 2.

The *SN* ratios were obtained by calculating the difference between the tensile properties and the indentation tensile properties. Since small error is desirable, a ''the-smaller-the-better type characteristic'' *SN* ratio was calculated by

$$SN = -10 \log\left[\frac{1}{\mathrm{x}}\sum_{i=1}^{\mathrm{x}} \mathrm{y}_i^2\right], \tag{7}$$

where x is the number of all data points and y_i is the value of the ith data point.

4.1 Number of Unloadings. The *SN* ratio is a maximum when the number of unloadings is ten times, as shown in Fig. 4. The *SN* ratio increases in the front part and vice versa. That means the number of unloadings has positive and negative effects simultaneously on the accuracy of the indentation tensile properties.

The several unloading stages are needed to calculate the indentation stiffness S in Eq. (3), which is used to calibrate the indentation depths; the calibrated indentation depths are used in Eq. (1) and Eq. (2) to obtain the true strain and the true stress. The number of unloadings is identical to the number of true stress-true strain pairs inserted in Eq. (5). Since the values of K and n in Eq. (5) are determined by logarithmic fit of the pairs, employing too few pairs is likely to yield unreliable values of K and n. Small variation in the logarithmic fit makes large scatter of the final results.

On the other hand, if there are too many pairs, many true stresses will be calculated in the low load range and the first unloading curve starts at too small indentation load because the unloadings are made at the same intervals. The true stress defined in Eq. (2) is based on the assumption that the deformation occurs in the fully plastic stage, and this assumption is not valid at low load ranges because the effects of elastic deformation can remain. According to the previous research [18], the fully plastic range begins at more than several kgf. Moreover, the load-depth curves in low load ranges cannot be reproduced because of limits of resolution on the load sensor and displacement sensor. Therefore, the true stresses obtained at low load ranges can be inaccurate, and there should be a certain optimum value for the number of unloadings, which is ten times in this study.

Table 2 Tensile properties of seven steels used here

Materials	Yield strength (MPa)	Tensile strength (MPa)	Work-hardening exponent	Uniform elongation
SCM400	605	955	0.182	0.0965
STD61	338	755	0.229	0.202
SK3	244	691	0.264	0.182
A335-P12	285	583	0.232	0.244
A335-P91	570	772	0.114	0.108
KP5	766	1003	0.123	0.0689
A106	334	670	0.222	0.156

4.2 Unloading Ratio. Figure 5 shows that the *SN* ratio decreases as the unloading ratio increases, which means that 30 percent is the optimum value of the unloading ratio in the 30 percent to 100 percent range. That means the unloading ratio affects the accuracy of the indentation tensile properties negatively and, therefore, a smaller value is preferred.

The unloading ratio means how much the load decreases at the unloading stage: for example, a 100 percent unloading ratio means

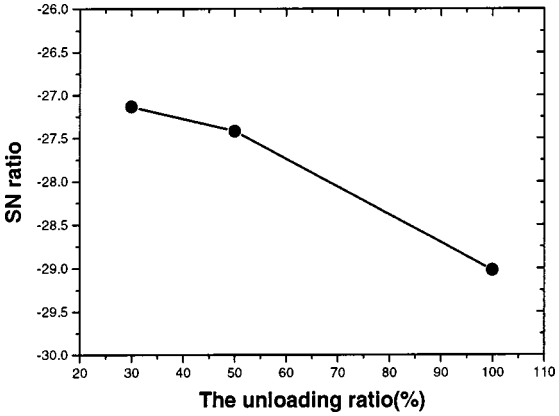

Fig. 5 *SN* ratio of the unloading ratio

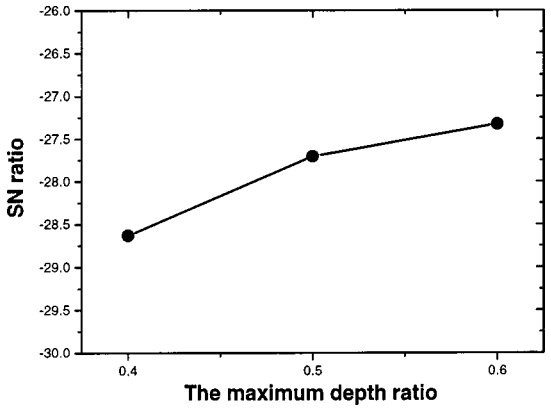

Fig. 6 *SN* ratio of the maximum depth ratio

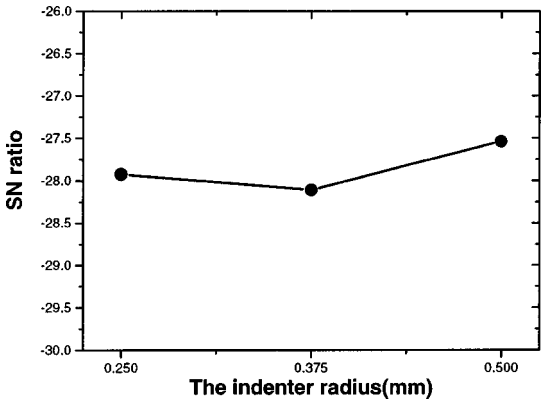

Fig. 7 *SN* ratio of the indenter radius

that the load decreases to zero. The unloading curve is used to calculate S. The unloading curve is expressed by a power-law fitting as [1]

$$P = k(h - h_f)^m, \tag{8}$$

where h is the indentation depth, and k, m, and h_f are determined by a least-squares fitting procedure. S is given by

$$S = \left(\frac{dP}{dh}\right)_{h=h_{max}} = mk(h_{max} - h_f)^{m-1}. \tag{9}$$

Since S is defined under the assumption of fully elastic recovery, the exact value of S cannot be calculated if the unloading curve contains the effects of plastic deformation. Marx and Balke [19] showed that a small unloading ratio is favorable for calculating an exact elastic modulus; this means that an unloading curve with small unloading ratio reflects elastic recovery better and eventually an exact S can be obtained. For these reasons, a small unloading ratio has positive effects on the SN ratio and the indentation tensile properties.

4.3 Maximum Depth Ratio. SN ratio increases as the maximum depth ratio increases from 0.4 to 0.5 and slowly increases from 0.5 to 0.6, as shown in Fig. 6. The optimum value in the 0.4–0.6 range is found to be 0.6. That means the maximum depth ratio has positive effects on the accuracy of the indentation tensile properties, and, therefore, a larger value is desired.

The maximum depth ratio is closely related to the true strain of Eq. (1). Thus, regardless of the indenter radius, the maximum value of the true strain is determined in terms of h_{max}/R, the maximum depth ratio, as follows:

$$\varepsilon_{max} = 0.12\sqrt{\frac{1}{1 - 2\left(\frac{h_{max}}{R}\right) + \left(\frac{h_{max}}{R}\right)^2} - 1}. \tag{10}$$

When the maximum depth ratio is 0.4, 0.5, and 0.6, the maximum strain is 0.160, 0.208, and 0.275, respectively. Many metals have maximum strains, also called uniform elongation, of about 0.2. Three metals of the seven metals used in this study have more than 0.160, and one metal more than 0.208. Since a maximum strain of 0.160 is insufficient to derive the stress-strain curves of metals and 0.208 is a little insufficient, a larger maximum depth ratio is preferred and there is some difference in the degrees of the SN ratio increase of the 0.4–0.5 range and the 0.5–0.6 range. However, an unreliable load-depth curve can be obtained more than 0.6 of the maximum depth ratio because the contact radius increases very slowly [20]. Therefore, 0.6 is the optimum value of the maximum depth ratio.

4.4 Indenter Radius. There is relatively little variation in the SN ratio for the indenter radius, as shown in Fig. 7, which means that the effects of the indenter radius may be negligible. The indenter radius is likely to determine the true strain as given in Eq. (1). However, the maximum strain is dependent only on the maximum depth ratio in Eq. (8), and this equation is identical to Eq. (1) if h_{max} is changed to h. The true strain is dependent only on the maximum depth ratio, which means the indenter radius has little effect on the true strain.

The indenter radius affects the range of the contact radius a in Eq. (2) by which the true stress is calculated. Materials tested by different indenter radii can be assumed to have identical maximum depth ratios and eventually identical true strains because the orthogonal table distributes the effects of each experimental parameter equally. Moreover, all materials experience the same deformation stages in the indenter radius range used in this study. According to plasticity theory, the same stresses should be measured in materials that have the same strain and the same deformation history. Thus, the indenter radius has little effect on the true stress. It is observed that the mean pressure related with the true stress in Eq. (2) increases rapidly in low load range or when the small indenters are used, which is called Indentation Size Effect (ISE). However, ISE is observed when the width of impression is below about fifty microns, which is much smaller than the width in this study [21]. For these reasons, the indenter radius has little effect on the true strain and the true stress, which make up the tensile curves. Therefore, the effects of the indenter radius can be negligible.

4.5 Evaluation of Indentation Tensile Properties With the Optimum Parameters. The indentation tensile properties of the seven steels were reevaluated with the optimum parameters, and compared with those with conventional parameters in Figs. 8(a–c). The diagonal lines in each figure mean that the indentation tensile properties are perfectly equal to the tensile properties from uniaxial tensile tests. The results with the optimum parameters (○) are closer to the diagonal lines than those with conventional parameters (●) for yield strength, tensile strength, and work-hardening exponent. Especially, much better results are observed for the materials with high work-hardening exponent. The accuracy of yield strength is improved 9.98 percent, tensile strength 3.36 percent and work-hardening exponent 13.0 percent better than the results with the conventional parameters. Moreover, it is observed that the divergences of the each indentation tensile property are much decreased.

Since the deformation of the material in the continuous indentation test is not a chemical reaction but a physical reaction, it is expected that there may be very little interaction. The final purpose of this study is to obtain the optimum parameters, which is not affected by the interaction. Therefore, though the interactions

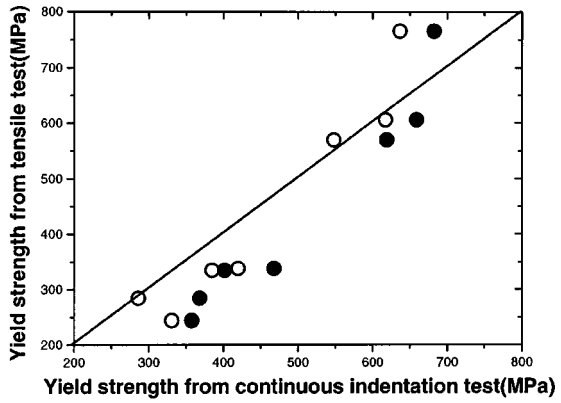

(a)

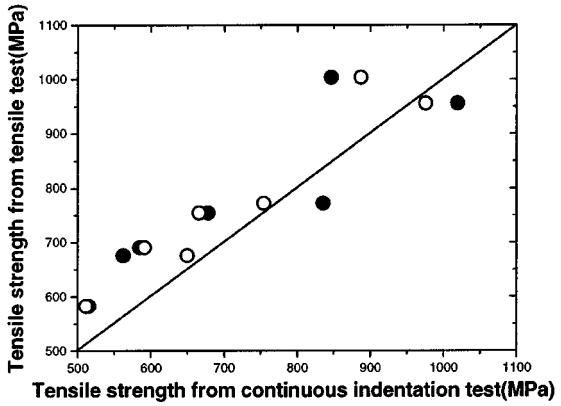

(b)

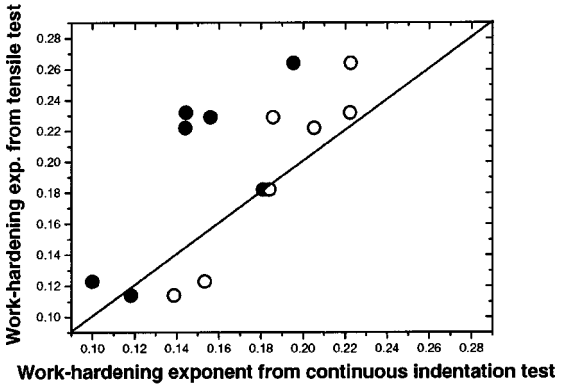

(c)

Fig. 8 Comparison between the indentation tensile properties (a) yield strength, (b) tensile strength, and (c) work-hardening exponent with the optimum parameters (○) and the conventional parameters (●)

among the experimental parameters were not considered in this study, it is proved that the optimum parameters determined by the Taguchi method are reasonable.

V Conclusions

The effects on the accuracy of indentation tensile properties and the optimum values of the number of unloadings and the unloading ratio, the maximum depth ratio and the indenter radius were analyzed quantitatively using the Taguchi method. It was found that:

(1) The indentation tensile properties vary with the experimental parameters that are included as variables in the numerical calculation procedures of the load-depth curves.

(2) The optimum experimental parameters were determined for evaluation of the indentation tensile properties by adapting the Taguchi method, one of design of experiment methods. Ten times, 30 percent and 0.6 were determined as the optimum values of the number of unloadings, the unloading ratio and the maximum depth ratio, respectively. The effects of the indenter radius can be negligible.

(3) The validity of the optimum parameters was confirmed. The indentation tensile properties with the optimum parameters were in better agreement with the tensile properties from uniaxial tensile tests than before.

Acknowledgment

This study was supported in part by the Korean Agency for Technology and Standards.

Nomenclature

a = contact radius
a_* = contact radius considering elastic deflection only
h = indentation depth
h_c^* = contact depth considering elastic deflection only
h_f = final depth
$h_{\max}$ = maximum depth
K = strength coefficient
k = fitting constant of unloading curve
m = exponent of unloading curve
n = work-hardening exponent
P = indentation load
$P_{\max}$ = maximum load
R = indenter radius
S = indentation stiffness
SN = signal-to-noise
x = number of all data
y_i = value of the ith data point
α = constant related with true strain
ε = true strain
$\varepsilon_{\max}$ = maximum strain
σ = true stress
Ψ = plastic constraint factor
ω = indenter geometry constant

References

[1] Oliver, W. C., and Pharr, G. M., 1992, "An Improved Technique for Determining Hardness and Elastic Modulus Using Load and Displacement Sensing Indentation Experiments," J. Mater. Res., **7**(6), pp. 1564–1583.
[2] Doerner, M. F., and Nix, W. D., 1986, "A Method for Interpreting the Data From Depth-Sensing Indentation Instruments," J. Mater. Res., **1**(4), pp. 601–616.
[3] Malzbender, J., and de With, G., 2000, "Energy Dissipation, Fracture Toughness and the Indentation Load-Displacement Curve of Coated Materials," Surf. Technol., **135**, pp. 60–68.
[4] Murty, K. L., Mathew, M. D., Wang, Y., Shah, V. N., and Haggag, F. M., 1998, "Nondestructive Determination of Tensile Properties and Fracture Toughness of Cold Worked A36 Steel," Int. J. Pressure Vessels Piping, **75**(11), pp. 831–840.
[5] Ahn, J.-H., and Kwon, D., 2001, "Derivation of Plastic Stress-Strain Relationship From Ball Indentation: Examination of Strain Definition and Pileup Effect," J. Mater. Res., **16**(11), pp. 3170–3178.
[6] Haggag, F. M., 1993, "In-Situ Measurements of Mechanical Properties Using Novel Automated Ball Indentation System," ASTM STP 1204, Philadelphia, PA, pp. 27–44.
[7] Asif, S. A. S., Wahl, K. J., and Colton, R. J., 1999, "Nanoindentation and Contact Stiffness Measurement Using Force Modulation With a Capacitive Load-Displacement Transducer," Rev. Sci. Instrum., **70**(3), pp. 2408–2413.
[8] Lucas, B. N., Oliver, W. C., and Swindeman, J. E., 1998, "The Dynamics of Frequency-Specific, Depth-Sensing Indentation Testing," *Fundamentals of Nanoindentation and Nanotribology*, N. R. Moody et al., eds., MRS, Warrendale, PA, **522**, pp. 3–14.
[9] Suresh, S., and Giannakopoulos, A. E., 1998, "A New Method for Estimating

Residual Stresses by Instrumented Sharp Indentation,'' Acta Mater., **46**(16), pp. 5755–5767.
[10] Lee, Y.-H., and Kwon, D., 2002, ''Residual Stresses in DLC/Si and Au/Si Systems: Application of a Stress-Relaxation Model to the Nanoindentation Technique,'' J. Mater. Res., **17**(4), pp. 901–906.
[11] Tabor, D., 1951, *Hardness of Metals*, Clarendon Press, Oxford, p. 2.
[12] Johnson, K. L., 1970, ''The Correlation of Indentation Experiments,'' J. Mech. Phys. Solids, **18**(2), pp. 115–126.
[13] Norbury, A. L., and Samuel, T., 1928, ''The Recovery and Sinking-in or Piling-up of Material in the Brinell Test, and the Effects of These Factors on the Correlation of the Brinell With Certain Other Hardness Tests,'' J. Iron Steel Inst., London, **117**, pp. 673–687.
[14] Hill, R., Storåkers, B., and Zdunek, A. B., 1989, ''A Theoretical Study of the Brinell Hardness Test,'' Proc. R. Soc. London, Ser. A, **423**, pp. 301–330.
[15] Dieter, G. E., 1989, *Mechanical Metallurgy*, McGraw-Hill, London, UK.
[16] Korean Standard B 0950, 2002, ''Metallic Materials—Instrumented Indentation Test for Indentation Tensile Properties,'' KSA, Seoul, Korea.
[17] Taguchi, G., 1987, *System of Experimental Design*, UNIPUB/Kraus International Pub., Millwood, NY, **1**, p. 165.
[18] Francis, H. A., 1976, ''Phenomenological Analysis of Plastic Spherical Indentation,'' Transaction of the ASME, pp. 272–381.
[19] Marx, V., and Balke, H., 1997, ''A Critical Investigation of the Unloading Behavior of Sharp Indentation,'' Acta Mater., **45**(9), pp. 3791–3800.
[20] Field, J. S., and Swain, M. V., 1995, ''Determining the Mechanical Properties of Small Volumes of Material From Submicrometer Spherical Indentations,'' J. Mater. Res., **10**(1), pp. 101–112.
[21] Begley, M. R., and Hutchinson, J. W., 1998, ''The Mechanics of Size-Dependent Indentation,'' J. Mech. Phys. Solids, **46**(10), pp. 2049–2068.